

# Reconfigurable Planar Monopole Antenna for Fifth-Generation Mobile Communication System

Peng Chen, Lihua Wang, and Zhonghua Ma

Information Engineering College  
Jimei University, Xiamen, Fujian, 361021, China  
chenpeng@jmu.edu.cn, liliya@jmu.edu.cn, mzhxm@jmu.edu.cn

**Abstract** — A frequency reconfigurable planar monopole antenna for fifth-generation (5G) mobile communication terminal equipment is presented. The proposed antenna uses a meandered monopole, branch resonance and other techniques to make the antenna resonant in multiple frequency bands. The antenna is compact in size (115 mm × 55 mm × 0.8 mm) and has a longitudinal length less than one-tenth of the resonant wavelength (working at 1.79 GHz). The pin diode is designed between the planar meandered monopole antenna and branch. The current path of the high-frequency current on the antenna can be easily controlled by controlling the DC bias voltage of the diode, and the operating frequency of the antenna is switched between three frequency bands. The antenna is fed directly through a 50 Ω matched transmission line. The measured data of the antenna in the anechoic chamber show good consistency with simulation data. The radiation pattern of the antenna shows good omnidirectional characteristics and good frequency characteristics, with a maximum radiation gain of 13.6 dBi. Experimental results demonstrate that the antenna can meet the design requirements of 5G communication.

**Index Terms** — 5G, branch-line coupler, frequency reconfigurability, planar monopole antenna.

## I. INTRODUCTION

With the maturity of fifth-generation (5G) communication technology, several new wireless communication bands have been approved for use, but the division of 5G frequency points in different countries and regions also presents a decentralized situation. Even limited to the sub-6 band, users need the ability to switch freely between dozens of frequency combinations for cross-border, cross-carrier network use.

Faced with the increasing requirement of frequency matching and frequency selection in terminal equipment, the design idea of blindly expanding antenna bandwidth to cover more frequency ranges has become increasingly more limited.

A typical example is that many scholars are

now realizing that UWB antennas used in UWB communications should be designed with frequency-specific notch points to be able to operate simultaneously with a wireless communication network and avoid interference by high-power wireless signals of the same frequency used in such a communication system [1–4].

Therefore, faced with the challenge of frequency switching, a frequency-reconfigurable antenna has become an alternative and solves the problem more effectively.

A large number of research results on frequency reconfigurable antennas exist [5–10]. Additionally, frequency-reconfigurable antennas have many advantages over traditional antennas, such as simplification and miniaturization, which can change the frequency [11–12].

A varactor diode and an external bias Tee structure were used in Ref. [13] to achieve flexible adjustment of the operating frequency band. A varactor diode combined with a bias circuit was also used in Ref. [14] to achieve dual-band frequency reconfiguration, and the monopole antenna has a lower profile. A sub-type patch structure and multiple PIN diodes were used in Ref. [15] to achieve coverage of three frequency bands from 1.45 to 4.52 GHz.

In this study, a frequency-reconfigurable planar monopole antenna that can be applied to 5G mobile communication terminal equipment is proposed.

Compared to the antenna described in Ref. [13], the frequency switching of the antenna described in this article through PIN diodes has low hardware cost, and its frequency-switching control method is simple. Compared with the antenna described in Ref. [14], the size of the low-profile monopole antenna proposed herein, applied to the low frequency at approximately 760 MHz, reaches 97 mm×97 mm×8 mm, its structure is more compact (28.3 mm×16.5 mm×0.8 mm), and its longitudinal length is less than one-tenth of the resonance wavelength. Compared with the antenna described in Ref. [15], the antenna described herein can support communication modes of more frequency bands, not only supporting 3G and 4G networks at the same

time, but also compatible with higher-frequency 5G communication networks, making the communication of mobile users more flexible and convenient.

## II. BASIC PROPOSED ANTENNA STRUCTURE

The proposed antenna is a planar monopole antenna that has been miniaturized by using meandered monopole antenna technology. The monopole in the form of a copper microstrip is realized by printed-circuit-board technology, and the meandering structure is designed on the limited plane, which reduces the length of the antenna to less than one-tenth of the maximum wavelength. The equal-width microstrip line forms an S-bend and is connected to the microstrip feeder that connects the SMA connector to the antenna. The slot of the S-shaped monopole antenna near the feeder is equivalent to that of the capacitor, and the capacitance can be adjusted by adjusting the structure parameter  $g$  to realize the matching between the antenna and feeder.

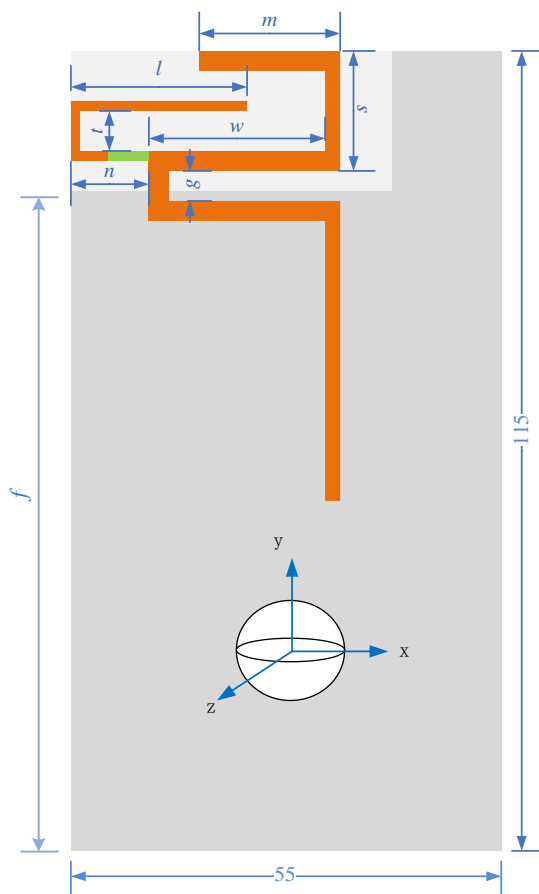


Fig. 1. Schematic of proposed antenna structure.

The structure of the proposed antenna is shown in Fig. 1, and a section of the U-shaped microstrip branch is connected with the S-shaped monopole antenna at the first bend. The connection is made by a PIN diode. The PIN diode used in the research are BAR50-02 of Infineon Company, which has low forward resistor, very low harmonics, and low capacitance at 0 V reverse bias at frequencies above 1 GHz (typ. 0.15 pF). It can work normally in 10 MHz–6 GHz. According to the PIN diode datasheet, the threshold voltage of 1.5V DC can control the ON-OFF state of the PIN diode. The diode represents a resistance of 3Ω for the ON state and a parallel circuit with a capacitance of 0.15 pF and a resistance of 5kΩ for the OFF state. When the diodes for the ON state has a low resistance which contribute to the insertion loss. According to the datasheet [16], the insertion loss is 0.27 dB.

By controlling the DC bias of the diode, it is easy to control the turning-on of the diode and realize the path reconstruction of the high-frequency current on the antenna surface, thus realizing the frequency control of the antenna.

To simulate the application environment, the antenna is designed on FR4 medium with an area of 115mm×55mm and thickness of 0.8 mm. The back of the antenna is covered with a large copper layer to simulate the integration of the antenna and circuit structure of the terminal equipment. The environmental parameters and structural parameters of the antenna are listed in Table 1.

Table 1: Parameters of antenna structure

Parameters	Value (mm)	Parameters	Value (mm)
$t$	5.8	$g$	1.7
$l$	19.4	$n$	7.7
$s$	11	$m$	25
$w$	17.5	$f$	100

The S-shaped monopole antenna with branches is equivalent to the circuit form shown in Fig. 2. The relationship between the branches and monopole antennas can be expressed as a parallel circuit. Branch and monopole antennas have different resonant frequencies because they have different current paths. The low-frequency radiation power is proportional to  $R_m$  and the high-frequency radiation power to  $R_b$ . The distributed capacitance introduced by the antenna is equivalent to that of  $C_a$  and the matching between the antenna and feeding circuit can be adjusted by controlling  $C_a$ . It is worth noting that the position relationship between the branch and the antenna is not reflected in the equivalent circuit; this part of the parameters also determines the antenna matching.

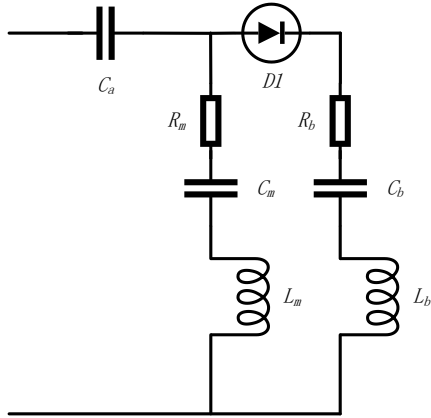


Fig. 2. Equivalent circuit of antenna.

The antenna has the advantages of simple structure, low process cost, and suitability for mobile terminal equipment. By controlling the DC bias of the diode, turning the diode on or off can be easily controlled and the antenna frequency can be reconfigured.

### III. PARAMETRIC STUDY OF FREQUENCY RECONFIGURABLE ANTENNA

When the PIN diode is off, since the diode reactance in the frequency band is very large, it is equivalent to a short-circuit state and the branch is equivalent to the meandering monopole antenna coupled patch. By adjusting the length of the planar meandering monopole antenna, the resonant frequency of the antenna can be changed, as shown in Fig. 3.

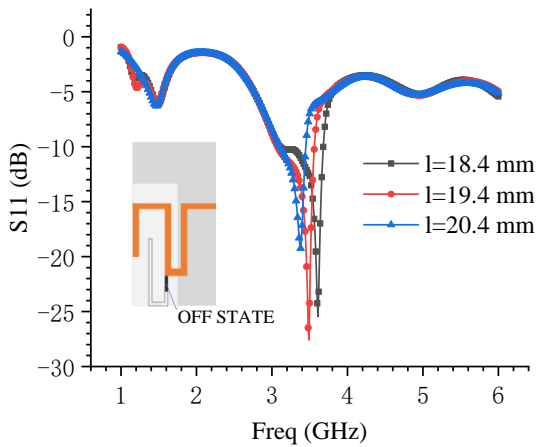


Fig. 3. Simulation results of antenna parameter  $S_{11}$ .

When the PIN diode is disconnected, here is an obvious resonance frequency point in the analysis frequency band, which corresponds to the arm length of the monopole antenna, When the arm length increases, the resonant frequency of the antenna moves to the low-

frequency band, and when it decreases the resonant frequency of the antenna moves to the high-frequency band. As shown in Fig. 3, the length of the monopole antenna arm can be changed by adjusting the structural parameters  $m$  and  $s$ , thereby controlling the antenna resonance frequency. When the structural parameters  $s$ ,  $w$ , and  $g$  are changed, the distributed capacitance of the antenna is also changed, and then the matching of the antenna changes.

According to a simulation analysis performed in Ansys HFSS software, when the PIN diode is disconnected and the antenna parameters are set as shown in Table 1, the impedance characteristics of the antenna are satisfactory. The impedance bandwidth ( $<-10$ dB) is 540MHz (3.07–3.61 GHz) and the relative bandwidth 16.2%, which can meet the requirement of 5G communication covering the (3.3–3.6)-GHz band.

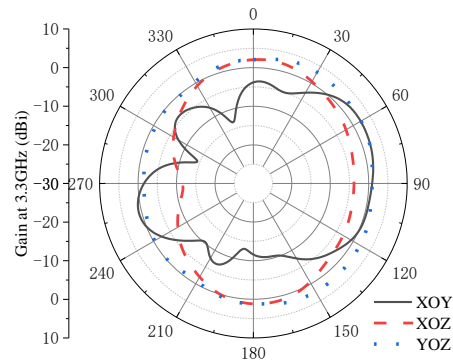


Fig. 4. Radiation pattern of proposed antenna when diode is off.

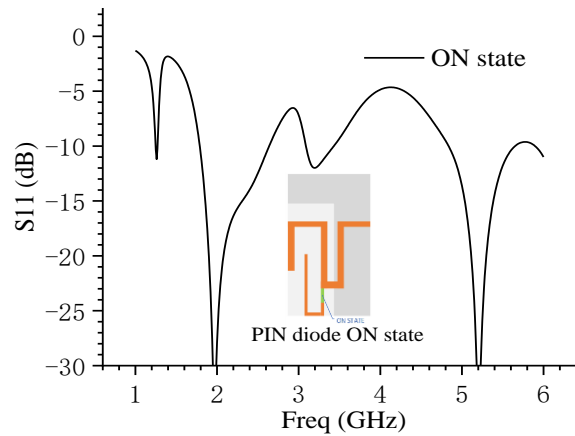


Fig. 5. Simulation results of antenna parameter  $S_{11}$ .

As shown in Fig. 4, the ZOZ and ZOY plane patterns fully exhibit isotropy when the antenna operates at a central frequency of 3.3 GHz in this frequency band. In the XOY plane pattern, the directivity of the antenna is largely strong, maximum direction of radiation points

to  $\varphi = 60^\circ$ , peak gain is 2.2 dBi, that of the corresponding back lobe level is  $-2.4$  dBi, and front-to-back ratio is 4.6 dB.

At a DC bias of 1.6 V for the PIN diode, the diode will be turned on. At this time, the diode is equivalent to a resistance of  $3 \Omega$  for the current in the frequency band. Owing to the access of the single branch, the surface current on the single arm of the monopole is shunted. A new shorter surface current path is formed, so the antenna shows two resonant frequency points on the band characteristic curve.

Similar to the analysis of the state of the diode, the resonant frequency of the high frequency can be controlled by adjusting the structural parameters  $t$ ,  $l$ , and  $n$ ; the analysis process is not redundant. It should be noted that, due to the conduction of the diode, the function of the U-shaped microstrip line in the antenna is changed from the coupling patch when the diode is off to the current branch of the monopole antenna, driving the low-frequency resonant point to a significantly lower frequency.

According to the simulation results in Ansys HFSS, the antenna shows dual-band characteristics when the diode is on, the frequency band ( $s_{11} < -10$  dB) of the antenna covers 1.79–2.63 and 4.827–5.66 GHz, and the relative bandwidth reaches 38% and 15.4%, respectively (Fig. 5). The coverage characteristics of the frequency band meet the requirements of DCS1800 (1710–1880MHz)/PCS1900 (1850–1990MHz)/UMTS2100 (1920–2170MHz)/LTE2300 (2350–2400MHz)/LTE2500 (2500–2690MHz) and the 5G communication frequency band of 4.8–5.0 GHz.

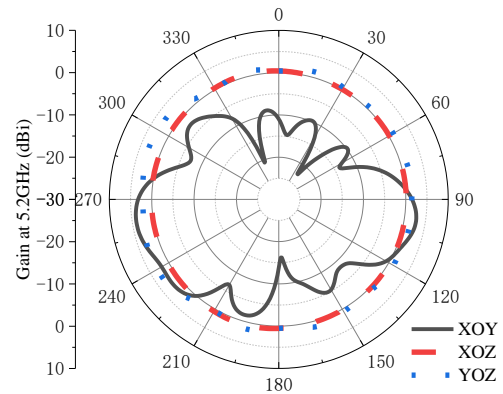
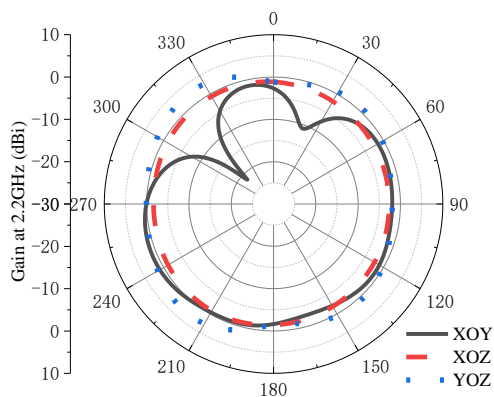
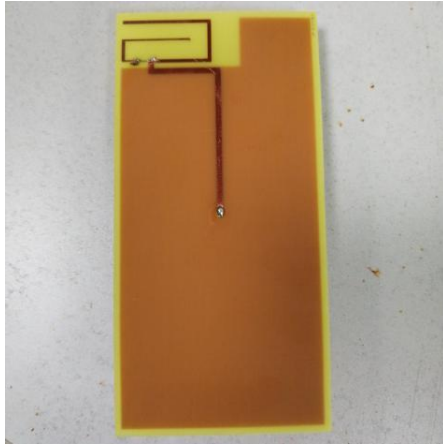


Fig. 6. Radiation pattern of proposed antenna when diode is on.

In terms of radiation characteristics, it can be seen from Fig. 6 that when the antenna operates at 2.2 GHz the antenna exhibits omnidirectional radiation characteristics in the YOZ and XOZ planes, and the XOY plane antenna shows good directivity with a maximum gain of 1.1 dBi. When the antenna operates at 5.2 GHz, the antenna shows omnidirectional radiation characteristics in the YOZ and XOZ planes, while the antenna shows good directivity with a maximum gain of 4.0 dBi. The stability of the multi-frequency pattern ensures that the devices using the antenna can switch between several working frequency bands.

#### IV. RESULTS AND ANALYSIS

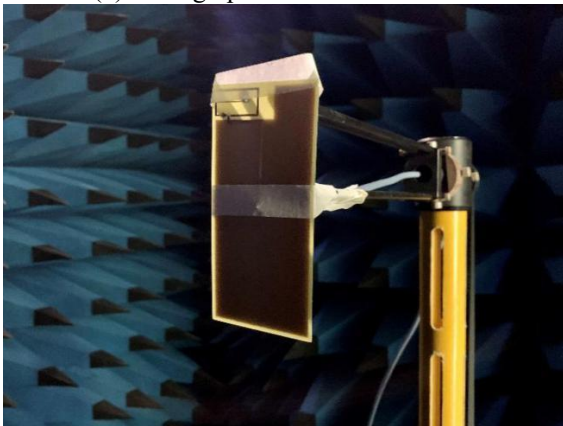
As shown in Fig. 7, the bias of the antenna can be supplied by battery or DC voltage source. During design, the power switch can be manually switched to achieve the function of switching the working frequency of the antenna, in the form of the realization that the product form will use the switch control circuit. The antenna is installed in the anechoic chamber and the antenna parameters measured. As shown in Fig. 8, the measured PIN diode can cover the frequency range from 3.1 to 4.8 GHz with a bandwidth of 1.7 GHz. Compared with the simulation results, the 3.5 GHz resonant point has better consistency, measured data have a lower reflection coefficient, and resonance performance at high frequency is more obvious, so a new resonant point is formed near 3.9 GHz; the bandwidth is enlarged relative to the simulation result under double resonance.



(a) Photograph of antenna front view



(b) Photograph of antenna rear view



(c) Proposed antenna being measured in anechoic chamber

Fig. 7. Proposed reconfigurable planar monopole antenna test photos.

As can be seen from Fig. 9, with the decrease of  $n$ , the bandwidth of the antenna obviously becomes smaller,

and the high frequency point and low frequency point produce frequency point offset. The size of  $f$  has a great influence on the performance of the antenna.

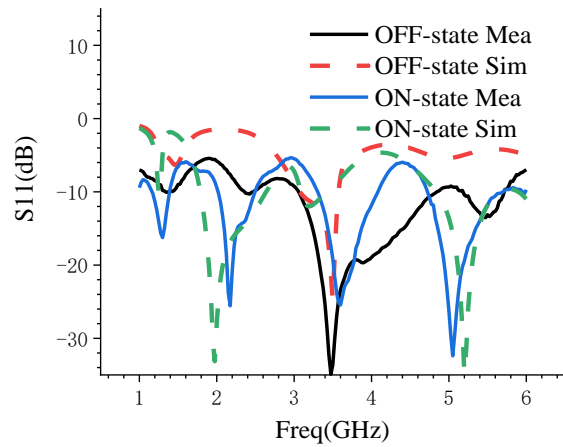


Fig. 8. Measured data of antenna parameter  $S_{11}$ .

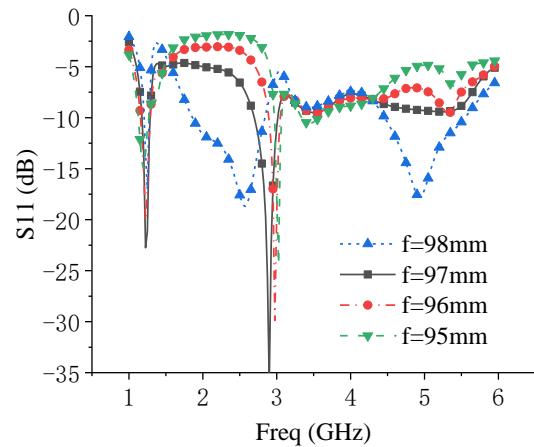
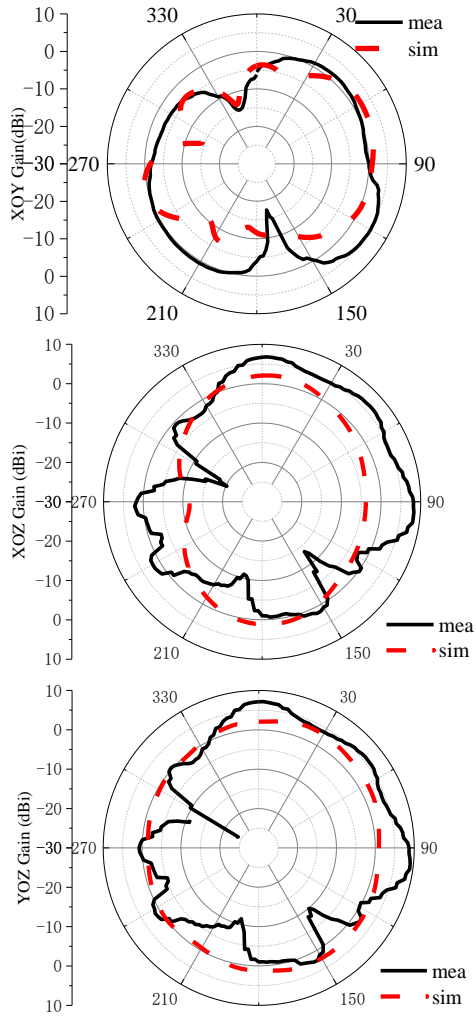
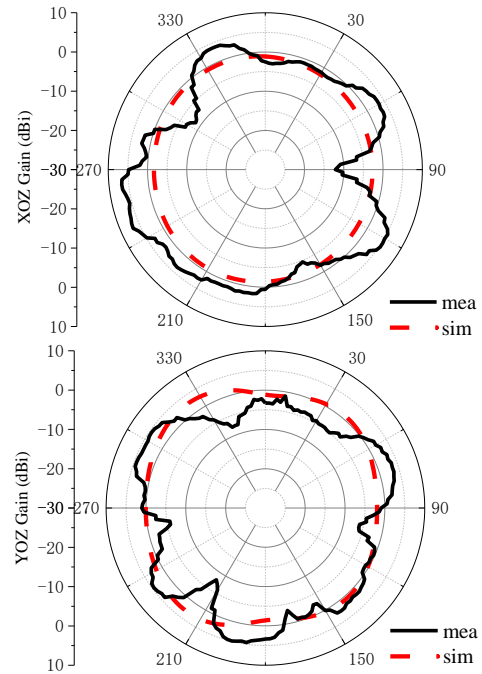
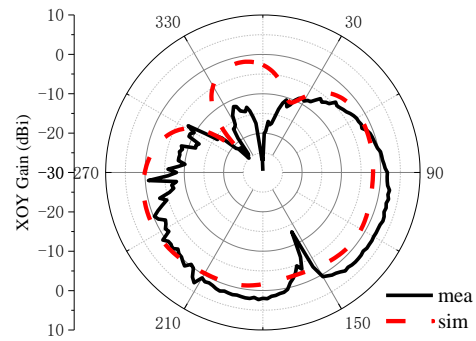


Fig. 9. Simulated reflection coefficients of the antenna for different  $n$ .

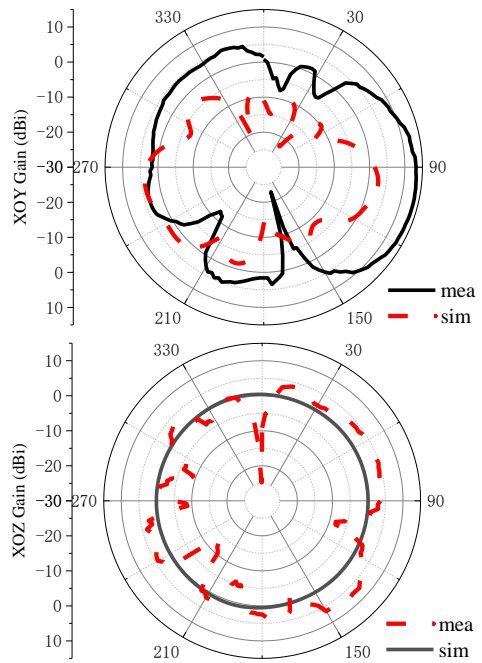
When the diode is on, the measured antenna can cover four frequency bands: 1.2–1.4, 2.0–2.5, 3.3–4.0, and 4.7–5.6 GHz. Compared with the simulation results, the coverage of the high-frequency band is closer, reflection coefficient of the low-frequency resonance relatively larger, and the low-frequency resonance point moves 200 MHz to the high-frequency part, which reduces the measured bandwidth by 200 MHz. However, the intermediate-frequency resonance points, which are not well matched in simulation, are also measured in experiment. The reason may be that the diode circuit is not more equivalent to the current distribution in the actual diode circuit.



(a) Radiation Pattern at 3.3 GHz (diode OFF-state)



(b) Radiation Pattern at 2.2 GHz (diode ON-state)



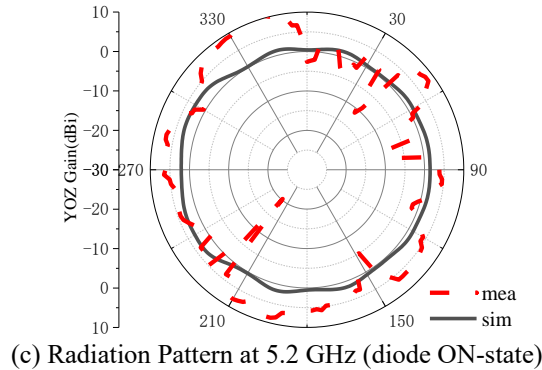


Fig. 10. Antenna multi-frequency working pattern.

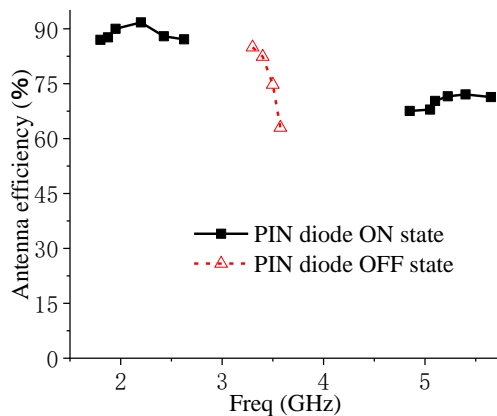


Fig. 11. Efficiency of the fabricated antenna at different frequency bands.

By switching the diode switch, the antenna can switch between three frequency bands easily. In three frequency bands, 2.2 GHz (diode ON), 3.3 GHz (diode OFF), and 5.2 GHz (diode ON) were selected to test the pattern.

According to the multi-frequency working pattern in Fig. 10, it can be seen that the radiation intensity in each direction of the three operating frequencies tested in the anechoic chamber exhibits little difference in the XOZ YOZ planes, and the omnidirectional characteristics are obvious; however, the directivity is stronger in the XOY plane. And the cross-polarization performance of the antenna is not ideal. The measured gains were 5.1 dBi (3.3 GHz), 2.7 dBi (2.2 GHz), and 13.6 dBi (5.2 GHz), respectively. The simulated antenna efficiency is shown in Fig. 11. As can be seen from the figure that the antenna efficiency is above 63% at different frequency bands. However, the efficiency of the antenna in the high frequency band is slightly reduced. Lower antenna efficiency is mostly due to the higher current flowing through the PIN diode.

Certainly, the error between the measured and simulated data needs further analysis, with the reasons for the error possibly caused by the following: First,

welding and PCB processing and other process errors; second, consistency error of the antenna's dielectric material and transmission line; and, third, analysis of the diode equivalent circuit, reduction degree of the simulation software, and systematic error of the testing instrument.

## ACKNOWLEDGMENT

This work was supported in the Fujian Natural Science Foundation Project (2020J02042 and 2019J01718) and the National Fund Training Project of Jimei University (ZP2021011).

## REFERENCES

- [1] C.-H. Lee, J.-H. Wu, C.-I. G. Hsu, H.-L. Chan, and H.-H. Chen, "Balanced band-notched UWB filtering circular patch antenna with common-mode suppression," *IEEE Antennas Wirel. Propag. Lett.*, vol. 16, pp. 2812-2815, Sept. 2017.
- [2] M. Elhabchi and M. N. Touahni, "CPW-fed miniaturized isosceles triangular slot UWB planar antenna with triple band-notched characteristics," *Prog. Srfi, and R. Electromagn. Res.*, vol. 87, pp. 59-66, 2019.
- [3] M. Rahman, M. NagshvarianJahromi, S. S. Mirjavadi, and A. M. Hamouda, "Compact UWB band-notched antenna with integrated bluetooth for personal wireless communication and UWB applications," *Electronics*, vol. 8, no. 2, Feb. 2019.
- [4] R. Sanyal, P. P. Sarkar, and S. Sarkar, "Octagonal nut shaped monopole UWB antenna with sextuple band notched characteristics," *AEU - Int. J. Electron. Commun.*, vol. 110, article ID 152833, Oct. 2019.
- [5] Y. He, W. Tian, and L. Zhang, "A novel dual-broadband dual-polarized electrical downtilt base station antenna for 2G/3G applications," *IEEE Access*, vol. 5, pp. 15241-15249, June 2017.
- [6] A. Chaugule, G. Mishra, and S. K. Sharma, "Investigations on frequency agile dual polarization dielectric lens high gain antenna," in *2016 IEEE International Symposium on Antennas and Propagation (APSURSI)*, article ID 16411953, pp. 837-838, June 2016.
- [7] Z. Nie, H. Zhai, L. Liu, J. Li, D. Hu, and J. Shi, "A dual-polarized frequency-reconfigurable low-profile antenna with harmonic suppression for 5G application," *IEEE Antennas Wirel. Propag. Lett.*, vol. 18, no. 6, pp. 1228-1232, June 2019.
- [8] Y. Li, W. Li, and Q. Ye, "A reconfigurable trip-notch-band antenna integrated with defected microstrip structure bandstop filter for ultra-wideband cognitive radio applications," *Int. J. Antennas Propag.*, vol. 2013, p. 13, article ID 472645, 2013.
- [9] A. Singh and C. E. Saavedra, "Fluidically

- reconfigurable MIMO antenna with pattern diversity for sub-6-GHz 5G relay node applications,” *Canadian Journal of Electrical and Computer Engineering-revue Canadienne Degenie Electrique Et Informatique*, vol. 43, no. 2, pp. 92-99, Spr. 2018.
- [10] M. M. Fakharian, P. Rezaei, and A. A. Orouji, “A multi-reconfigurable CLL-Loaded planar monopole antenna,” *Radioengineering*, vol. 29, no. 2, pp. 313-320, June 2018.
- [11] S. F. Jilani, A. Rahimian, Y. Alfadhl, and A. Alomainy, “Low-profile flexible frequency-reconfigurable millimetre-wave antenna for 5G applications,” *Flex. Print. Electron.*, vol. 3, no. 3, p. 035003, Aug. 2018.
- [12] Y.-L. Tsai and J.-H. Chen, “Design of a dual-polarized beam-switching antenna for small base station application,” in *2015 International Workshop on Electromagnetics: Applications and Student Innovation Competition (iWEM)*, article ID 15681179, Nov. 2015.
- [13] I. Ben Trad, I. Rouissi, J.-M. Floch, and H. Trabelsi, “Frequency reconfigurable multiband planar antenna with wide tuning frequency range,” in *2016 10th European Conference on Antennas and Propagation (EuCAP)*, article ID 16037660, Apr. 2016.
- [14] N. Nguyen-Trong, A. Piotrowski, and C. Fumeaux, “A frequency-reconfigurable dual-band low-profile monopolar antenna,” *IEEE Trans. Antennas Propag.*, vol. 65, no. 7, pp. 3336-3343, July 2017.
- [15] Y. K. Choukiker and S. K. Behera, “Wideband frequency reconfigurable Koch snowflake fractal antenna,” *IET Microw. Antennas Amp Propag.*, vol. 11, no. 2, pp. 203-208, Jan. 2017.
- [16] Datasheet for Infineon BAR50-02V, Silicon PIN Diode, Infineon Technologies AG, 18 Sep. 2011. Available at <http://www.farnell.com/datasheets/1500311.pdf>.